

Chapter 11

Rescue Echocardiography

Byron Ferguson, MD and Joshua Zimmerman, MD, FASE

Abstract Current recommendations include the use of transesophageal echocardiography (TEE) for acute, persistent, unexplained hypotension. Perioperative transesophageal echocardiography is well suited to assess for the etiology of acute hemodynamic instability as it provides information on multiple aspects of cardiovascular physiology, from contractility and valvular function to volume status and intracardiac pressures. Its portable and relatively noninvasive nature allows quick diagnosis and rapid implementation of therapy in unstable patients. A rapid, qualitative assessment of the hemodynamic event, or “eyeballing”, is the cornerstone to rescue echocardiography. Rescue echocardiography is a process, not an event, where a qualitative estimation of the abnormality followed by reevaluation after the intervention is suggested. This chapter describes this process of rapid diagnosis, intervention, and reevaluation and highlights several key and common causes of perioperative hemodynamic instability.

Keywords Rescue echocardiography • Hemodynamic instability • Transesophageal echocardiography • Hypotension • Valvular disease • Ventricular dysfunction • Hypovolemia • Tamponade

Electronic supplementary material The online version of this chapter (doi:[10.1007/978-3-319-34124-8_11](https://doi.org/10.1007/978-3-319-34124-8_11)) contains supplementary material, which is available to authorized users.

B. Ferguson, MD (✉)
Department of Anesthesiology, University of California San Diego,
200 W Arbor Drive MC #8770, San Diego, CA 92103, USA
e-mail: bfergerson@ucsd.edu; byronfergerson@gmail.com

J. Zimmerman, MD, FASE
Department of Anesthesiology, University of Utah,
30 N 1900 E, Salt Lake City, UT 84132, USA
e-mail: Joshua.Zimmerman@hsc.utah.edu

The American Society of Echocardiography (ASE) recommends the use of transesophageal echocardiography (TEE) for acute, persistent, unexplained hypotension [1]. Transesophageal echocardiography is well suited to assess for the etiology of acute hemodynamic instability as it provides information on multiple aspects of cardiovascular physiology, from contractility and valvular function to volume status and intracardiac pressures. There are several other key advantages as well. It is portable, relatively noninvasive, and provides a qualitative picture of the hemodynamic event. A rapid, qualitative assessment of the hemodynamic event, or “eyeballing”, is the cornerstone to rescue echocardiography. A detailed quantitative analysis of cardiovascular function is neither feasible nor necessary in the emergent setting. Grasping the overarching hemodynamic picture, performing an intervention, and reassessing the hemodynamics is the most practical and effective use of TEE. A qualitative analysis is also significantly easier to learn [2].

Unfortunately, there is a paucity of data on the use of TEE in the setting of hemodynamic instability in the perioperative period. Markin et al. looked retrospectively at 364 rescue echocardiograms performed on cardiac and noncardiac cases throughout the perioperative period [3]. Anesthetic management was changed in more than half of the patients evaluated by TEE with no echo-related complications. Interestingly, there was a change in surgical management in 7 % of the cases.

Time is of the essence in rescue echocardiography as the etiology of the instability must be rapidly diagnosed and acted upon. There are 28 recommended views in the most recently published comprehensive TEE exam, many of which are redundant. Redundancy is valuable in general because it allows for visualization of structures from multiple angles. It is not, however, conducive to brevity. For this reason, a condensed examination is suggested. The “rescue exam” presented in this chapter is a modification of the 11 cross-sectional views recommended by the ASE and Society of Cardiovascular Anesthesiologists (SCA) for the basic TEE exam [4]. The primary differences are the order of the views and the use of spectral Doppler. Spectral Doppler is vital to delineate between certain causes of hemodynamic instability and thus is included in this exam. The rescue exam is short but covers the majority of clinically relevant pathologies. In addition, performing the same exam every time minimizes distraction. The rescue exam is listed in Table 11.1, beginning in the mid-esophagus and ending in the stomach for ease of use. Similar protocols have been studied and used effectively [3, 5, 6]. In agreement with the ASE and SCA [4], it is suggested to perform and store the limited exam in its entirety before focusing on segments specific to the area of interest.

It is important to note that rescue echocardiography is a process, not an event. The cardiovascular system is complex and dynamic, potentially changing on a beat-to-beat basis. What may be considered an appropriate intervention one minute, may not be appropriate the next. It may be difficult to discern the precise cause of the cardiovascular abnormality. In addition, it is possible that multiple abnormalities are present. Similar to Markin et al. [3], a qualitative estimation—a “best guess”—of the abnormality followed by reevaluation after the intervention is suggested. If parameters improve, one should continue the intervention. If they do not improve or worsen, an alternate diagnosis should be sought.

Table 11.1 Recommended limited TEE exam

-
1. Mid-esophageal AV SAX
 2. Mid-esophageal AV LAX
 - Measurement of LVOT diameter
 3. Mid-esophageal bicaval
 4. Mid-esophageal RV inflow/outflow
 5. Mid-esophageal 4 chamber
 - With and without CFD on the TV and MV
 6. Mid-esophageal 2 chamber
 7. Mid-esophageal LV LAX
 8. Transgastric midpapillary LV SAX
 9. Deep transgastric LAX
 - PWD of LVOT
 - Calculation of stroke volume
 10. Descending aorta SAX
-

AV Aortic valve; *SAX* Short axis; *LAX* Long axis; *CFD* Color flow Doppler; *TV* Tricuspid valve; *MV* Mitral valve; *PWD* Pulse wave Doppler; *RV* Right ventricle; *LV* Left ventricle; *LVOT* Left ventricular outflow tract; *TG* Transgastric

The most common causes of hemodynamic instability will be reviewed: acute valvular and aortic pathology, tamponade, RV dysfunction, pulmonary embolism, hypovolemia, low afterload, and LV hypo- and hypercontractility.

Acute Valvular and Aortic Pathology

The echocardiographic assessments of valvular and aortic pathology (specifically dissection and traumatic rupture) are discussed elsewhere in the text and will be mentioned only briefly here (see Chaps. 7 and 10). Acute valvular dysfunction is most likely to occur on left-sided structures [7]. Endocarditis is the most common cause of acute regurgitation. Other potential causes include trauma, aortic dissection, and left ventricular ischemia. Evaluation of valvular regurgitation in the acute setting should be limited to a rapid, qualitative assessment as quantitative measures may be inaccurate [7]. Color flow Doppler (CFD) is the primary modality for a visual assessment of the regurgitant jet focusing primarily on the vena contracta. New onset or a change in chronic regurgitation is more valuable than grading the severity. Keep in mind that the regurgitation may be a manifestation of changes in ventricular function and loading conditions induced by another cardiac abnormality.

Regarding aortic dissection, as discussed in Chap. 10, TEE is as reliable as helical computed tomography and magnetic resonance imaging in diagnosing or ruling out a dissection [8]. The diagnosis of dissection is based on the detection of an intimal flap that divides the aorta into true and false lumens [9]. The lumens are best delineated through CFD. TEE is also valuable in assessing for the intimal tear, intramural hematomas [10], and penetrating ulcers [11].

Cardiac Tamponade

Cardiac Tamponade

2D	<ul style="list-style-type: none"> Echolucent space between heart and pericardium (may be loculated) Effusion >2cm are severe Chamber Collapse (RA – Systolic; RV – Diastolic)
CFD	<ul style="list-style-type: none"> Typically not utilized
Spectral	<ul style="list-style-type: none"> >10% respiratory variation in LVOT VTI

RA = right atrium; RV = right ventricle; LVOT = left ventricular outflow tract; VTI = velocity time integral

Pericardial effusions with associated tamponade physiology are extremely dangerous under general anesthesia. Rapid diagnosis and intervention is necessary making echocardiography, with its portability and accuracy, the diagnostic modality of choice. Acute effusions are generally due to trauma or ischemia, but must also be considered in the setting of inflammation, infection, malignancy, and renal and hepatic failure. Pericardial effusions are seen as darkened areas between

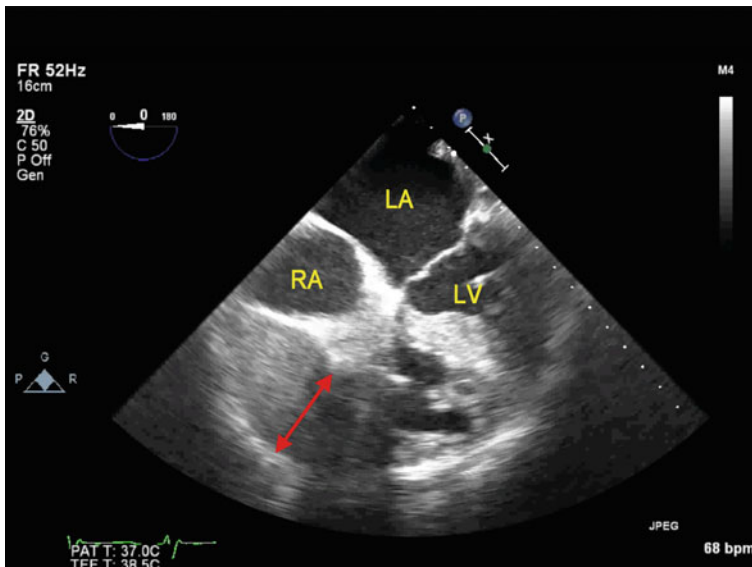


Fig. 11.1 Mid-esophageal four-chamber view demonstrating an acute pericardial effusion following percutaneous transvenous lead extraction. Double-headed red arrow indicates the pericardial effusion. LA Left Atrium; LV Left Ventricle; RA Right Atrium

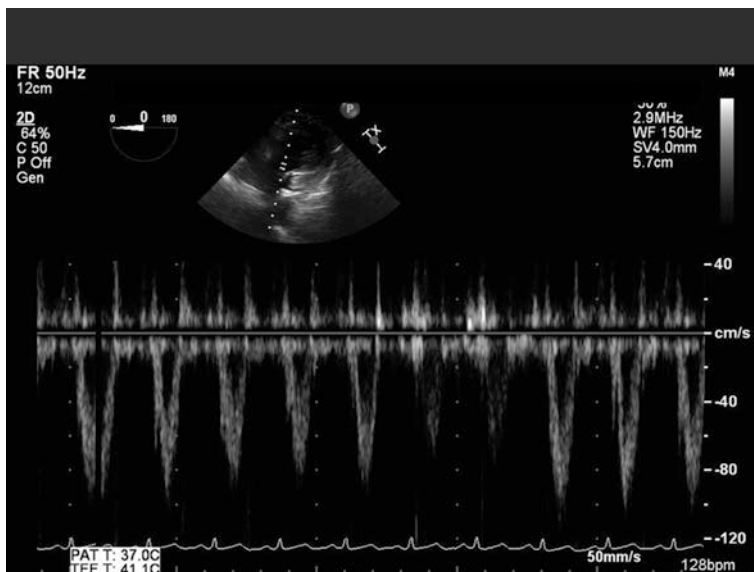


Fig. 11.2 Deep transgastric long axis view with pulse wave Doppler placed in the left ventricular outflow tract showing respiratory variability

the heart and the parietal layer of the pericardium (Fig. 11.1; Video 11.1). An effusion may be identified in nearly any mid-esophageal or transgastric view. Effusions measuring less than 1 cm are considered small; 1–2 cm are considered moderate; and >2 cm are considered large. Visualization of an effusion does not necessarily mean there is tamponade physiology. The pericardium can become quite distensible in the setting of a chronic effusion and thus, have a limited effect on intracardiac pressures and filling. However, in the case of extreme hemodynamic instability, a large pericardial effusion should be considered to cause cardiac tamponade regardless of the results of the continuing study (i.e., chamber collapse or spectral Doppler findings). A pericardial effusion can be contained within a loculation making it difficult to locate. The localized pressure exerted on the heart in this situation can still cause cardiac tamponade.

Echocardiographic diagnosis of cardiac tamponade is based on both two-dimensional and spectral Doppler findings. The normal respiratory variation in LV stroke volume (SV) seen during mechanical ventilation is exaggerated in the setting of tamponade physiology with SV increasing on inspiration and decreasing on expiration (see below for a detailed discussion of the physiology of this variation). The variation can be detected by pulse wave Doppler interrogation of the left ventricular outflow tract in the deep transgastric view using a sweep speed of 25–50 mm/sec (Fig. 11.2). Sweep speed indicates how fast the spectral Doppler refreshes on the screen (a lower speed allows the visualization of more beats per

Table 11.2 Respiratory variation in LV outflow in the setting of tamponade

	Mechanical ventilation	
	Inspiration	Expiration
LV Outflow	↑	↓

screen). A respiratory variation greater than 10 % in the LV outflow tract is one of the initial echocardiographic signs of cardiac tamponade (Table 11.2).

Further fluid accumulation in the pericardial space will soon cause the pericardial pressure to exceed right atrial (RA) pressure. This will be visualized as a late diastolic collapse of the RA which will extend into systole (Fig. 11.3; Video 11.2). The mid-esophageal RV inflow/outflow and the mid-esophageal four chamber are the best views to visualize this. As the pericardial pressure increases further, the RV will begin to collapse in diastole. The RV outflow tract is most likely to collapse and thus the preferred view is the RV inflow–outflow. The thicker left-sided structures are less likely to collapse. When left-sided collapse is seen, this portends a bad outcome. Once the diagnosis is established, echocardiography can be a useful adjunct to guide needle placement during a pericardiocentesis [12]. Table 11.3 outlines the two-dimensional manifestations of tamponade.

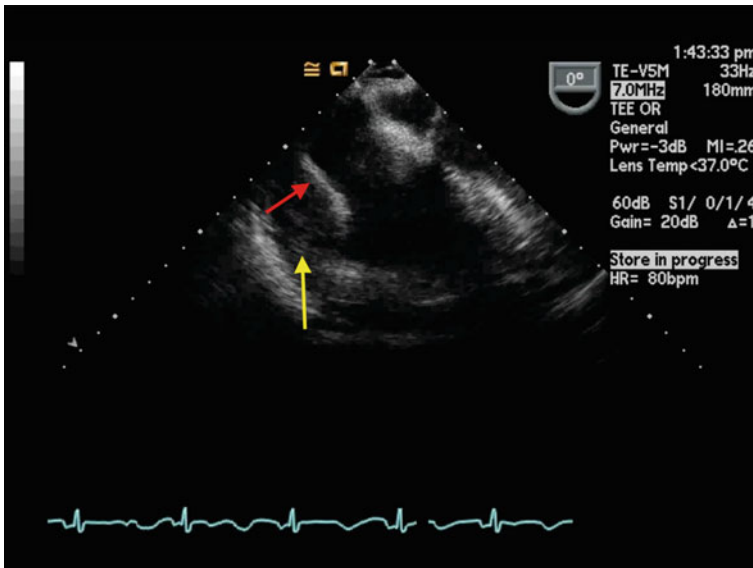


Fig. 11.3 Mid-esophageal four-chamber view with right atrial collapse in the setting of a pericardial effusion indicating tamponade physiology. *Red arrow* indicates right atrial systolic free wall collapse. *Yellow arrow* indicates the pericardial effusion

Table 11.3 Two dimensional manifestations of cardiac tamponade

	Systole		Diastole	
	Normal	Tamponade	Normal	Tamponade
RA	Expansion	Compression	Contraction	Contraction
RV	Contraction	Contraction	Expansion	Compression

RA Right Atrium; RV Right Ventricle

Right Ventricular Dysfunction

Right Ventricular Dysfunction	
2D	<ul style="list-style-type: none"> • RA & RV Size (RV should be 2/3 size of LV) • Encroachment of RV into LV • “D-shaped” LV (flattened septum) • Reduced TAPSE
CFD	<ul style="list-style-type: none"> • New or worsened TR (dilated annulus)
Spectral	<ul style="list-style-type: none"> • PASP estimation

RA = right atrium; RV = right ventricle; LV = left ventricle; TAPSE = tricuspid annular plane systolic excursion; TR = tricuspid regurgitation

Right ventricular failure (please also see Chap. 8) is the inability of the RV to provide adequate blood flow to the LV in the setting of a normal central venous pressure. RV failure in cardiac and noncardiac surgeries has a very high mortality [13]. Potential causes of RV failure are numerous but generally involve RV contractile dysfunction in association with acute elevations in pulmonary artery pressures [14]. The anatomy of the RV is complex making echocardiographic assessment very difficult [15]. For this reason, we suggest performing a qualitative assessment in the emergent setting. A qualitative assessment of RV function is as good as MRI at detecting dysfunction [16]. Evaluation begins with inspection of right-sided chambers looking for dilation of the RV and RA. Mid-esophageal four-chamber, RV inflow–outflow, bicaval as well as transgastric midpapillary short axis views are helpful in evaluating the right heart. Encroachment into the left side with right-to-left bowing of the interatrial septum (Fig. 11.4; Video 11.3) and/or a “D-shaped” intraventricular septum seen in the transgastric midpapillary short axis view (Fig. 11.5; Video 11.4) indicate elevated right-sided pressures. RV contractility can then be assessed by looking for regional wall motion abnormalities. In addition, one can qualitatively evaluate the distance the tricuspid annulus moves down in systole (tricuspid annular systolic excursion or TAPSE) [17] (Fig. 11.6). A reduced TAPSE less than 17 mm suggests RV dysfunction [18]. Lastly, new onset or worsening of chronic tricuspid regurgitation may indicate either RV contractile dysfunction or annular dilation.

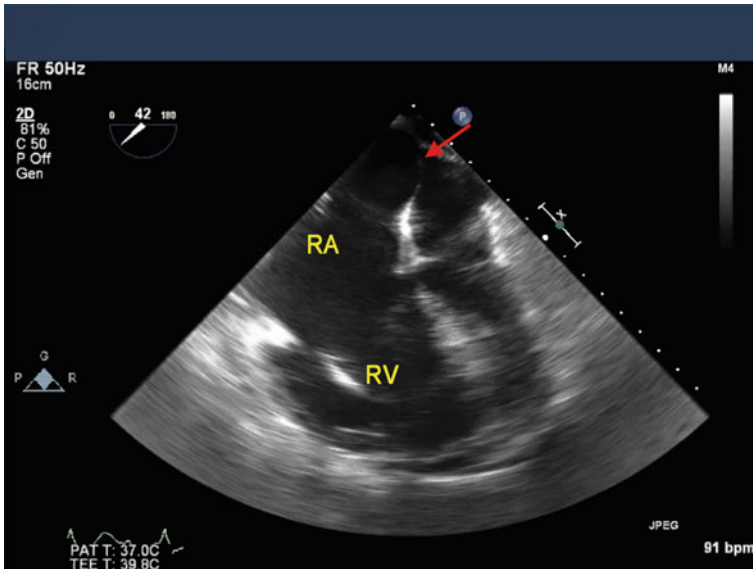


Fig. 11.4 Mid-esophageal four-chamber view of a patient with right heart failure. The *red arrow* indicates the atrial septal bowing due to high right atrial pressure. RA Right Atrium; RV Right Ventricle

Pulmonary Embolism

Pulmonary Embolism

2D	<ul style="list-style-type: none"> • Evidence of RV Failure • Dilated RA and RV • Evidence of thromboembolic material in right heart (Main or Right PA) • McConnell’s sign – hypokinetic RV with normal RV apical function
CFD	<ul style="list-style-type: none"> • New or worsened TR (dilated annulus)
Spectral	<ul style="list-style-type: none"> • PASP estimation

RA = right atrium; RV = right ventricle; TR = tricuspid regurgitation

Early diagnosis and treatment can reduce the mortality associated with a pulmonary embolism (PE) tenfold [19]. Although TEE can help guide both diagnosis and management, it is not the gold standard [20]. Echocardiography has a high specificity and a low sensitivity (90 and 56 % respectively) [21]. Risk factors associated with PE are listed in Table 11.4.

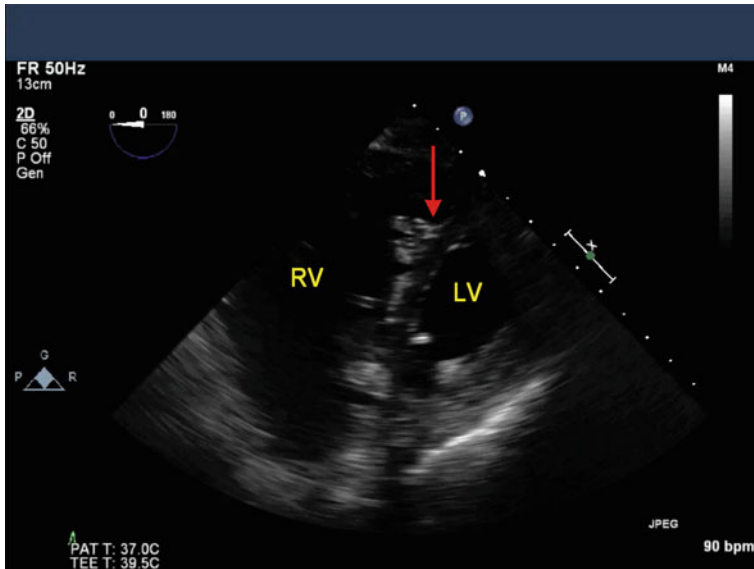


Fig. 11.5 Transgastric midpapillary short axis view revealing a “D” shaped interventricular septum secondary to right ventricular failure. *Red arrow* indicates flattened interventricular septum. *RV* Right Ventricle; *LV* Left Ventricle

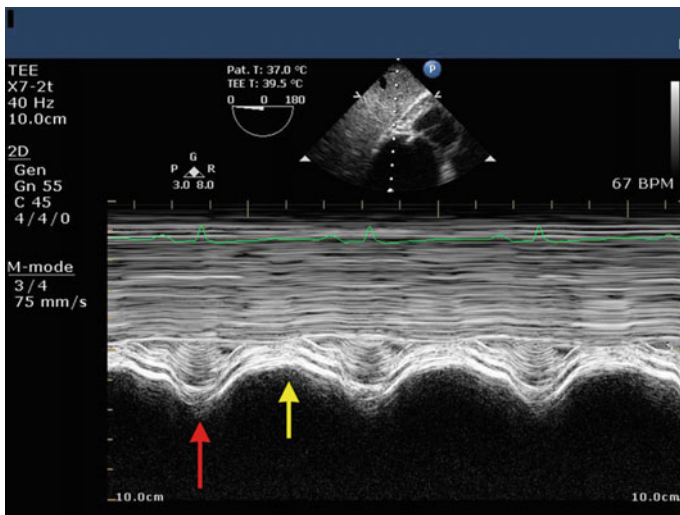


Fig. 11.6 Example of tricuspid annular plane systolic excursion (TAPSE) using M-mode imaging of the tricuspid annulus in the transgastric right ventricular inflow view. *Red arrow* indicates tricuspid annulus in diastole, while the *yellow arrow* indicates the tricuspid annulus in systole. The difference in position is the TAPSE measurement

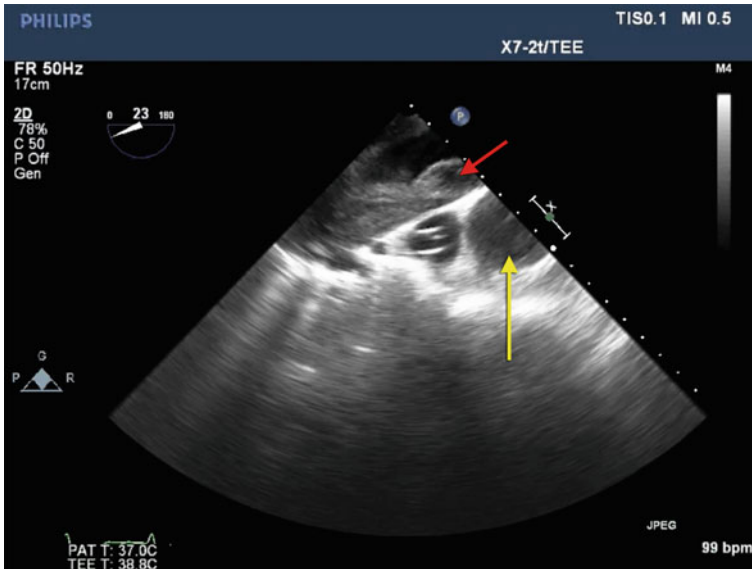


Fig. 11.7 Mid-esophageal ascending aortic short axis view with slight probe rotation to the right. Thrombus noted in the right pulmonary artery (*red arrow*). *Yellow arrow* indicates the ascending aorta in short axis

Table 11.4 Risk factors associated with pulmonary embolism

-
- Malignancy
 - Prolonged immobilization
 - Obesity
 - Tobacco use
 - Medications particularly
 - Oral contraceptives
 - Hormone replacement therapy
 - Antipsychotics
 - General Surgery particularly
 - Hip fractures
 - Acute spinal cord injuries
 - Trauma
-

A thrombus can be found anywhere on the right side from the vena cavae to the pulmonary artery (PA) and can be seen in over 80 % of cases (Fig. 11.7; Video 11.5). The ideal views to assess for thrombus include the mid-esophageal bicaval, RV inflow–outflow, and ascending aorta short axis. The main and right PAs can be seen by withdrawal of the probe to the high esophagus until a cross section of the ascending aorta is obtained. The left PA, on the other hand, is often obscured by the tracheobronchial tree.

Although a thrombus visualized in a right-sided cardiac structure is pathognomonic of PE, right ventricular wall motion abnormalities are the most common echocardiographic findings [20]. The extent of RV dysfunction correlates with the clot burden [22, 23] and overall mortality [24–26]. McConnell et al. showed that a hypokinetic RV free wall and a normal to hyperdynamic apex has a sensitivity of 77 % and a specificity of 94 % in predicting a PE [27]. Subsequent studies, however, have found a reduced sensitivity and specificity [28]. Structural and inflammatory changes in the LV associated with a PE as well as reduced coronary perfusion from loss of SV can lead to LV dysfunction. A low LV ejection fraction is an independent predictor of mortality in the setting of acute PE [24].

Left Ventricular Dysfunction

Left Ventricular Dysfunction	
2D	<u>Regional</u> • Wall Motion Abnormalities (Thickening and Excursion) <u>Global</u> • FAC or EF • LV or LA dilation • SEC <u>LVOTO</u> • Movement of anterior MV leaflet during systole (SAM) • Hyperdynamic, hypovolemic LV
CFD	<u>Regional / Global</u> • New or worsened MR (dilated annulus vs papillary dysfunction) <u>LVOTO</u> • New anterior MR jet from anterior MV displacement into LVOT (SAM) Aliasing in LVOT
Spectral	<u>Regional / Global</u> • Decreased SV or CO (calculated from LVOT) <u>LVOTO</u> • “Dagger” shaped – late peaking high velocity CWD profile

FAC = Fractional Area of Change; *EF* = Ejection Fraction; *LV* = left ventricle; *LA* = left atrium; *SEC* = spontaneous echo contrast; *SAM* = systolic anterior motion; *MR* = mitral regurgitation; *MV* = mitral valve; *LVOT* = left ventricular outflow tract; *SV* = stroke volume; *CO* = cardiac output; *CWD* = continuous wave Doppler; *LVOTO* = Left Ventricular Outflow Tract Obstruction

Echocardiography is an excellent tool for the diagnosis and management of LV dysfunction, particularly in the setting of myocardial ischemia. Segmental wall thickening less than 30 % suggests myocardial ischemia and can manifest within seconds making it an earlier marker of ischemia than ECG changes [29–31]. Acute ischemia is distinguished from chronic by a change in segmental wall motion from

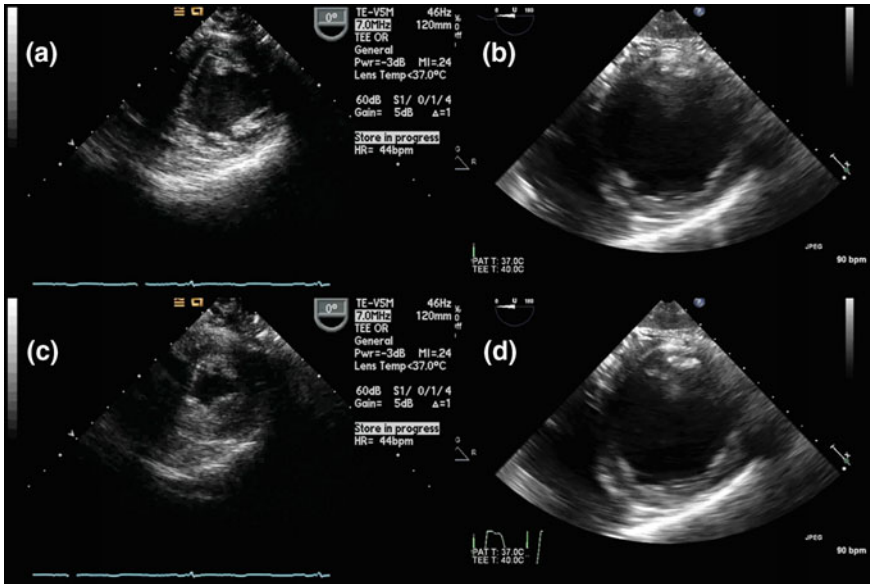


Fig. 11.8 Comparison of normal versus poor ejection fraction using the transgastric midpapillary short axis view. **a** and **c** are the diastolic and systolic frames, respectively, of a patient with normal systolic function. **b** and **d** are the diastolic and systolic frames, respectively, of a patient with grossly abnormal systolic function

baseline by two grades (i.e., from normal to severe hypokinesia) in two or more segments (Video 11.6) [32]. Stress, inflammation, and catecholamine excess associated with acute illness can also cause secondary cardiomyopathies and LV dysfunction [33]. Sepsis-induced cardiomyopathy [33] and stress-induced cardiomyopathy, also known as Takotsubo cardiomyopathy, [34] are relatively common causes of nonischemic LV dysfunction. Regardless of etiology, the echocardiographic manifestations of LV dysfunction are similar.

In keeping with the concept of a qualitative echocardiographic assessment in the setting of hemodynamic instability, the SCA recommends an estimation of the LV ejection fraction when assessing who may benefit from inotropic therapy [4]. Visual estimation, or “eyeballing”, has been found to be as good as Simpson’s biplane method [35] and 3D echocardiography [36] and requires only approximately 20 studies to become proficient [37]. The transgastric midpapillary short axis (SAX) view is the primary view used for assessing LV contractility (Fig. 11.8; Video 11.7). A reduced fractional area change (FAC), which is the comparison of the end-diastolic area (EDA) and end-systolic area (ESA), indicates poor LV function. An FAC is calculated by using the equation $(LVEDA - LVESA) / LVEDA$ with normal values being approximately the same as those for EF (Fig. 11.9; Video 11.8) [38]. It is important to note, however, that with regional dysfunction, the transgastric midpapillary short axis view may miss significant pathology in the basal and apical segments [39]. A brief assessment of the LV in the

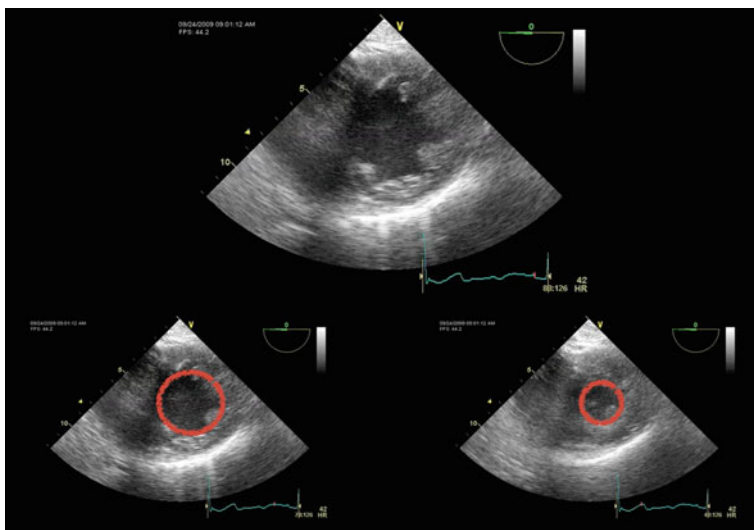


Fig. 11.9 Example of how to calculate left ventricular fractional area change. The image on the *top* is the transgastric short axis. The image on the *bottom left* is a rough estimate of the end-diastolic area. The image on the *bottom right* is a rough estimate of the end-systolic area. Fractional area change is then a percentage change between the two areas

four-chamber, two-chamber, and long axis views looking for segmental wall motion abnormalities will aid in diagnosis. Particular attention should be paid to the apex as it contributes a significant portion of the overall EF (Video 11.9).

Left ventricular hypercontractility resulting in dynamic left ventricular outflow tract obstruction (LVOTO) may also cause hemodynamic instability and must be considered in patients with risk factors whose hemodynamics worsen with inotropic support. LVOTO can occur in many pathophysiologic settings (Table 11.5). LVOTO likely results from localized increases in flow velocity during ejection due to a narrow LVOT. This results in the anterior mitral leaflet and chordae being

Table 11.5 Pathophysiologic settings associated with left ventricular outflow tract obstruction

-
- Hypertrophic cardiomyopathy
 - Hypertension [56]
 - Type 1 diabetes [57]
 - Myocardial ischemia [58, 59]
 - Pheochromocytoma [60]
 - Takotsubo cardiomyopathy [61, 62]
 - Valvular replacements and repairs [63, 64]
 - Catecholamine administration [65, 66]
-

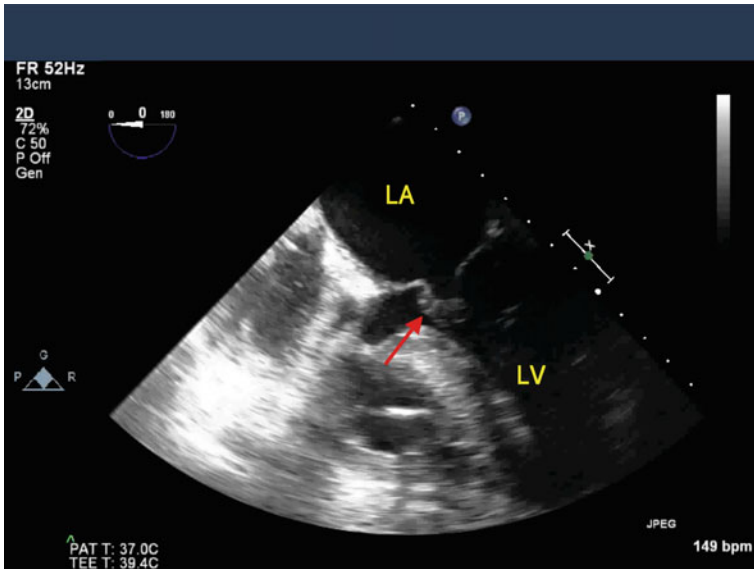


Fig. 11.10 Midesophageal four-chamber view in systole of a patient with left ventricular outflow tract obstruction. Note the anterior mitral leaflet contacting the septum (*Red Arrow*). LA Left Atrium; LV Left Ventricle

drawn toward the septum [40, 41], causing mid-to-late systolic mitral regurgitation and LVOT obstruction. It is often possible to see movement of the anterior leaflet of the MV toward the upper septum in the ME Four Chamber or ME LAX views (Fig. 11.10; Video 11.10). Color flow Doppler (CFD) may show an anteriorly directed MR jet as well as turbulent flow in the LVOT. A “dagger” shaped spectral Doppler pattern in the LVOT is the hallmark echocardiographic finding in LVOTO. Obstruction occurs late in systole because it takes time for the blood to generate enough velocity to draw in the mitral apparatus via Venturi effect. This dynamic property of the obstruction yields a late peaking continuous wave Doppler (CWD) pattern producing a “dagger” shape (Fig. 11.11). This profile shape is distinctly different from the fixed obstruction of aortic valve stenosis (see Chap. 7). The peak velocity of the wave will be high consistent with an elevated pressure gradient.

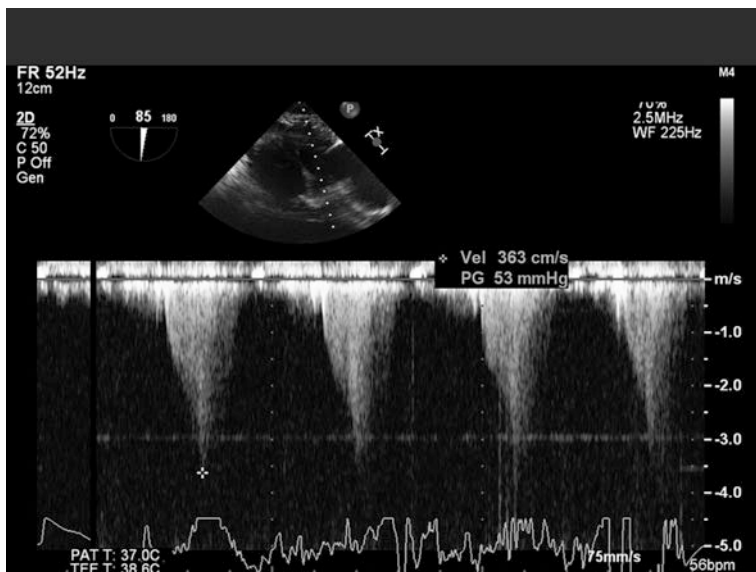


Fig. 11.11 Pulse wave Doppler in the left ventricular outflow tract revealing a “dagger” shaped wave consistent with dynamic outflow obstruction

Hypovolemia

Hypovolemia	
2D	<ul style="list-style-type: none"> • Small end-diastolic area / Small end-systolic area • Hyperdynamic LV
CFD	<ul style="list-style-type: none"> • Typically not utilized
Spectral	<ul style="list-style-type: none"> • Decreased SV or CO (calculated from LVOT) • Respiratory variation of peak LVOT velocity > 12 %

LV = left ventricle; *SV* = stroke volume; *CO* = cardiac output; *LVOT* = left ventricular outflow tract

The transgastric midpapillary short axis view has been shown to be a reasonable view for estimating ventricular volume by assessments of the LV end-diastolic (LVEDA) and end-systolic (LVESA) areas [42–44]. A euvolemic patient has a “normal” LVEDA, whereas the LVEDA of a hypovolemic patient is often reduced because of a reduced expansion (Fig. 11.12; Video 11.11). Normal value ranges for LVEDA is 8–14 cm² [45]. Several studies have confirmed the correlation between LV volume and LVEDA [46–49], although at varying strengths of correlation.

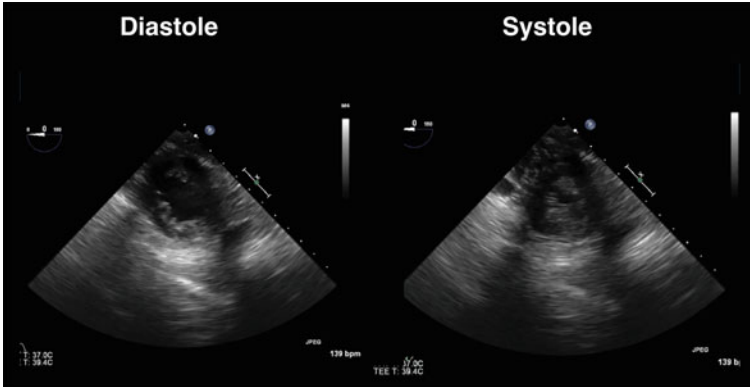


Fig. 11.12 Diastolic and Systolic frames from a transgastric midpapillary short axis view in the setting of hypovolemia. Note the small end-diastolic and end-systolic areas

The LVESA reflects the end point of the LV ejection fraction (EF). A hypovolemic patient who starts off with a reduced LV diastolic volume (and thus a reduced LVEDA) will end with a reduced systolic volume (and thus reduced LVESA). A correlation between a reduced LVEDA and hypovolemia has also been established [50]. Evaluation of the LVEDA and LVESA aid in qualitatively assessing volume status but often require further evaluation to confirm.

A reduced stroke volume (SV) in the setting of a normal or hyperdynamic LV strongly suggests hypovolemia as a cause of hypotension. Calculation of stroke volume assumes a cylindrical LVOT. The area of the cylinder is determined by measuring the LVOT diameter and using the following equation:

$$\text{Area} = D^2 \times 0.785$$

The LVOT diameter is usually measured in the mid-esophageal long axis view approximately 5 mm proximal to the aortic valve (Fig. 11.13). Small inaccuracies in measuring the diameter can introduce significant errors in the overall calculations since the diameter is squared. For this reason it is important to use the same LVOT diameter annular measurement for all subsequent calculations when performing serial SV measurements.

The length of the cylinder is determined by calculating the average distance a red blood cell travels in the LVOT during ejection, also called the stroke distance. Using the deep transgastric view, the pulse wave Doppler cursor is placed in the LVOT and a systolic waveform is obtained. The waveform is the velocities (i.e., speed and direction) of the red blood cells in the LVOT over time. The stroke distance, also called the velocity time integral (VTI), is obtained by tracing the Doppler wave (Fig. 11.14). To better understand this concept, consider a car traveling 50 miles an hour for 2 h. Figure 11.15 illustrates this data plotted on a graph with velocity on the Y-axis and time on the X-axis. The area of the rectangle

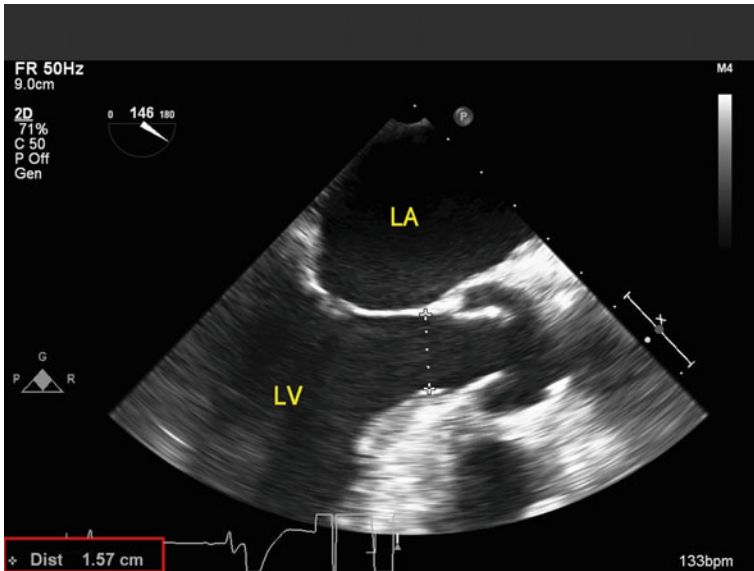


Fig. 11.13 Example of how to measure the diameter of the left ventricular outflow tract in the mid-esophageal long axis view. *LA* Left Atrium; *LV* Left Ventricle

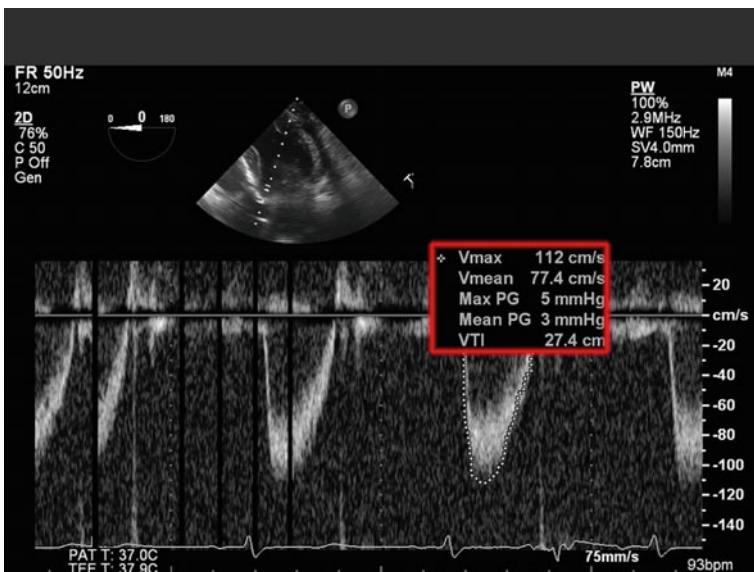


Fig. 11.14 Spectral profile from pulse wave Doppler placed in the left ventricular outflow tract in a Deep transgastric long axis view. Tracing the profile provides the velocity time integral (stroke distance)

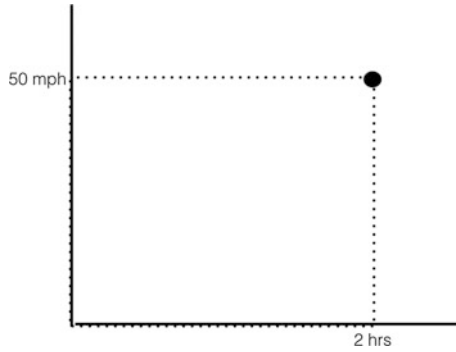


Fig. 11.15 Area under the curve for a time/velocity graph

created by these measurements yields a distance (i.e., $50 \text{ mph} \times 2 \text{ h} = 100 \text{ miles}$). The VTI is similar to this calculation in that it is the area under the curve of red blood cell velocities over time. In this case, the velocities are represented by centimeters per second, the time by seconds, and the VTI by centimeters.

The overall equation for determining the SV is the following (Fig. 11.16):

$$SV = D^2 \times 0.785 \times VTI$$

Cardiac output (CO) can then be calculated by multiplying SV by the heart rate (HR). This method of stroke volume calculation is the recommended method for determining CO by the American Society of Echocardiography [51].

Fig. 11.16 LVOT stroke volume calculation (Area of LVOT \times Stroke Distance)



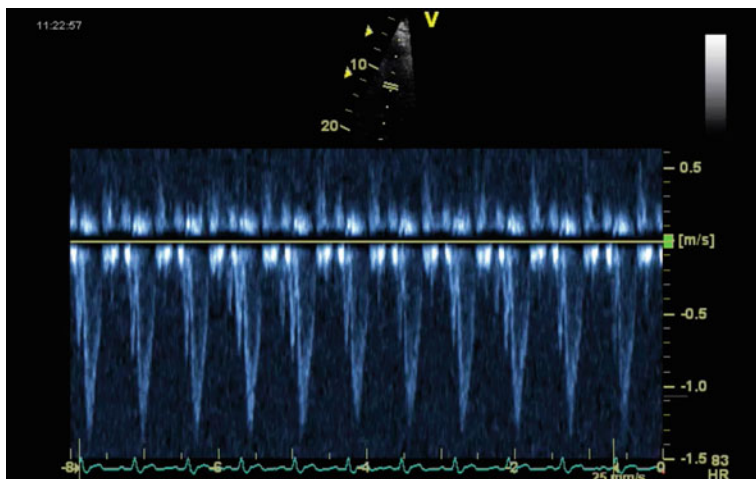


Fig. 11.17 Pulse wave Doppler in the left ventricular outflow tract showing minimal change in velocity with respiration

In addition to a static calculation of SV, volume status can be determined by dynamic changes in SV with respiration. Dynamic indices assess fluid responsiveness, which is the effect of a change in preload on SV [52]. Positive pressure insufflation pushes blood out of the lungs into the LV augmenting LV SV. At the same time, the positive intrathoracic pressure reduces RV preload and increases RV afterload thus reducing RV stroke volume. After several beats, the reduced RV stroke volume results in a reduced LV preload and reduced LV SV. These changes are exaggerated when the ventricles are on the steep part of the Frank–Starling curve with the magnitude of this variation predicting fluid responsiveness. Pulse wave Doppler interrogation of the LVOT over time has been shown to accurately assess these changes in SV and thus predict fluid responsiveness [53] (Fig. 11.17). One can use the following equation to quantitatively determine fluid responsiveness [54]:

$$\Delta V_{\text{peak}}(\%) = 100 \times (V_{\text{max}} - V_{\text{min}}) / [(V_{\text{max}} + V_{\text{min}}) / 2]$$

V_{min} represents the minimum velocity in the LVOT and V_{max} the maximum velocity. A ΔV_{peak} of 12 % or greater indicates volume responsiveness with a sensitivity of 100 % and specificity of 89 %. Such a calculation is impractical in the emergent setting. A visual estimate of the respiratory variation is often adequate (normal LVOT variation is <15 %).

Low Afterload

Low Afterload	
2D	<ul style="list-style-type: none"> • Normal end-diastolic area / Small end-systolic area • Hyperdynamic LV
CFD	<ul style="list-style-type: none"> • Typically not utilized
Spectral	<ul style="list-style-type: none"> • Elevated SV or CO (calculated from LVOT)

LV = left ventricle; *SV* = stroke volume; *CO* = cardiac output; *LVOT* = left ventricular outflow tract

Theoretically, the LVEDA and LVESA, typically measured in the transgastric midpapillary short axis view, can also help determine if the patient has a low afterload. A euvolemic patient should have a normal LVEDA regardless of afterload. If the afterload is low, the EF should increase which manifests as a small LVESA. Therefore, a euvolemic patient with a low afterload should have a normal LVEDA but a reduced LVESA (Fig. 11.18; Video 11.12). In contrast, a hypovolemic patient with a normal afterload should have a reduced LVEDA and LVESA. Table 11.6 compares LVEDAs and LVESAs in hypovolemia and low afterload. Unfortunately, a direct relationship between a low afterload and a normal LVEDA with a low LVESA has not been established in the literature, only suggested [50, 55]. A qualitative assessment of the LVEDA and LVESA can therefore only suggest hypovolemia or low afterload. Further confirmation by way of calculating the stroke volume, as described above, is often necessary. The stroke volume

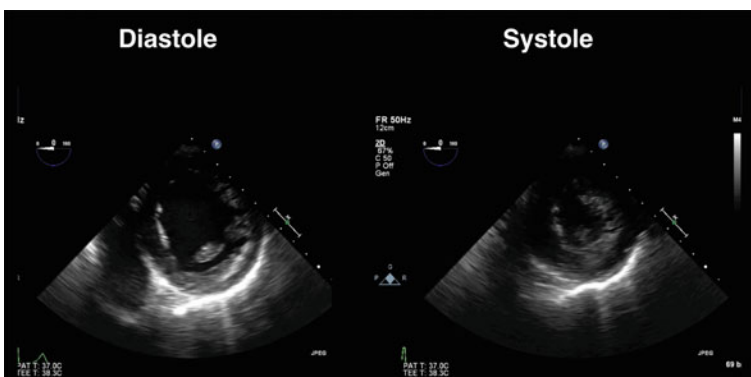


Fig. 11.18 Transgastric midpapillary short axis view with evidence of low afterload (small end-systolic area and normal end-diastolic area)

Table 11.6 Left ventricular end-diastolic and systolic areas in the setting of hypovolemia and low afterload

	LVEDA	LVESA
Normal	NI	NI
Low afterload	NI	Reduced
Hypovolemia	Reduced	Reduced

LVEDA Left Ventricular end-diastolic area; *LVESA* Left ventricular end-systolic area; *NI* Normal

should be elevated in the setting of a low afterload and reduced in the setting of hypovolemia.

Conclusion

Echocardiography is extremely useful to the perioperative physician in assessing the cause of hemodynamic instability, aiding in both diagnosis and management. It is the diagnostic tool of choice owing to its portability and ease of use. Not only does TEE help identify etiology, it also allows the practitioner to follow the effects of an intervention and make changes if necessary.

References

1. American Society of A, Society of Cardiovascular Anesthesiologists Task Force on Transesophageal E. Practice guidelines for perioperative transesophageal echocardiography. An updated report by the American Society of Anesthesiologists and the Society of Cardiovascular Anesthesiologists Task Force on Transesophageal Echocardiography. *Anesthesiology*. 2010;112(5):1084–96.
2. Price S, Ilper H, Uddin S, et al. Peri-resuscitation echocardiography: training the novice practitioner. *Resuscitation*. 2010;81(11):1534–9.
3. Markin NW, Gmelch BS, Griffie MJ, Holmberg TJ, Morgan DE, Zimmerman JM. A review of 364 perioperative rescue echocardiograms: findings of an anesthesiologist-staffed perioperative echocardiography service. *J Cardiothorac Vasc Anesth*. 2015;29(1):82–8.
4. Reeves ST, Finley AC, Skubas NJ, et al. Basic perioperative transesophageal echocardiography examination. *Anesth Analg*. 2013;117(3):543–58.
5. Miller JP, Lambert AS, Shapiro WA, Russell IA, Schiller NB, Cahalan MK. The Adequacy of Basic Intraoperative Transesophageal Echocardiography Performed by Experienced Anesthesiologists. *Anesthesia and Analgesia*. 2001:1103–10.
6. Shillcutt SK, Markin NW, Montzingo CR, Brakke TR. Use of rapid “rescue” perioperative echocardiography to improve outcomes after hemodynamic instability in noncardiac surgical patients. *J Cardiothorac Vasc Anesth*. 2012;26(3):362–70.
7. Stout KK, Verrier ED. Acute valvular regurgitation. *Circulation*. 2009;119(25):3232–41.
8. Shiga T, Wajima Zi, Apfel CC, Inoue T, Ohe Y. Diagnostic accuracy of transesophageal echocardiography, helical computed tomography, and magnetic resonance imaging for suspected thoracic aortic dissection. *Arch Intern Med*. 2006;166(13):1350.

9. Evangelista A, Flachskampf FA, Erbel R, et al. Echocardiography in aortic diseases: EAE recommendations for clinical practice. *Eur J Echocardiogr.* 2010;11(8):645–58.
10. Erbel R, Oelert H, Meyer J, et al. Effect of medical and surgical therapy on aortic dissection evaluated by transesophageal echocardiography. Implications for prognosis and therapy. The european cooperative study group on echocardiography. *Circulation.* 1993;87(5):1604–15.
11. Vilacosta I, San Román JA, Aragoncillo P, et al. Penetrating atherosclerotic aortic ulcer: documentation by transesophageal echocardiography. *J Am Coll Cardiol.* 1998;32(1):83–9.
12. Salem K, Mulji A, Lonn E. Echocardiographically guided pericardiocentesis—The gold standard for the management of pericardial effusion and cardiac tamponade. *Can J Cardiol.* 1999;15(11):1251–5.
13. Denault AY, Haddad F, Jacobsohn E, Deschamps A. Perioperative right ventricular dysfunction. *Curr Opin Anaesthesiol.* 2013;26(1):71–81.
14. Zochios V. Does β_2 -agonist use improve survival in critically ill patients with acute respiratory distress syndrome? In: *Reducing mortality in critically ill patients.* Springer Science+Business Media; 2015. pp. 103–9.
15. Sheehan F, Redington A. The right ventricle: anatomy, physiology and clinical imaging. *Heart.* 2008;94(11):1510–5.
16. Drake D, Gupta R, Lloyd SG, Gupta H. Right ventricular function assessment: comparison of geometric and visual method to short-axis slice summation method. *Echocardiography.* 2007;24(10):1013–9.
17. Lang RM, Bierig M, Devereux RB, et al. Recommendations for chamber quantification: a report from the american society of echocardiography's guidelines and standards committee and the chamber quantification writing group, developed in conjunction with the european association of echocardiography, a branch of the European society of cardiology. *J Am Soc Echocardiogr.* 2005;18(12):1440–63.
18. Lang RM, Badano LP, Mor-Avi V, et al. Recommendations for cardiac chamber quantification by echocardiography in adults: an update from the American Society of Echocardiography and the European Association of Cardiovascular Imaging. *J Am Soc Echocardiogr.* 2015;28(1):1–39, e14.
19. Tapson VF. Acute pulmonary embolism. *N Engl J Med.* 2008;358(10):1037–52.
20. Visnjevac O, Pourafkari L, Nader ND. Role of perioperative monitoring in diagnosis of massive intraoperative cardiopulmonary embolism. *J Cardiovasc Thorac Res.* 2014;6(3):141–5.
21. Miniati M, Monti S, Pratali L, et al. Value of transthoracic echocardiography in the diagnosis of pulmonary embolism: results of a prospective study in unselected patients. *Am J Med.* 2001;110(7):528–35.
22. Kjaergaard J, Schaadt BK, Lund JO, Hassager C. Quantification of right ventricular function in acute pulmonary embolism: relation to extent of pulmonary perfusion defects. *Eur J Echocardiogr.* 2008;9(5):641–5.
23. Ribeiro A, Juhlin-Dannfelt A, Brodin L-Å, Holmgren A, Jorfeldt L. Pulmonary embolism: relation between the degree of right ventricle overload and the extent of perfusion defects. *Am Heart J.* 1998;135(5):868–74.
24. Kjaergaard J, Schaadt BK, Lund JO, Hassager C. Prognostic importance of quantitative echocardiographic evaluation in patients suspected of first non-massive pulmonary embolism. *Eur J Echocardiogr.* 2009;10(1):89–95.
25. Ribeiro A, Lindmarker P, Juhlin-Dannfelt A, Johnsson H, Jorfeldt L. Echocardiography Doppler in pulmonary embolism: right ventricular dysfunction as a predictor of mortality rate. *Am Heart J.* 1997;134(3):479–87.
26. Sanchez O, Trinquart L, Colombet I, et al. Prognostic value of right ventricular dysfunction in patients with haemodynamically stable pulmonary embolism: a systematic review. *Eur Heart J.* 2008;29(12):1569–77.
27. McConnell MV, Solomon SD, Rayan ME, Come PC, Goldhaber SZ, Lee RT. Regional right ventricular dysfunction detected by echocardiography in acute pulmonary embolism. *Am J Cardiol.* 1996;78(4):469–73.

28. Lodato JA, Ward RP, Lang RM. Echocardiographic predictors of pulmonary embolism in patients referred for helical CT. *Echocardiography*. 2008;25(6):584–90.
29. Hauser AM, Gangadharan V, Ramos RG, Gordon S, Timmis GC, Dudlets P. Sequence of mechanical, electrocardiographic and clinical effects of repeated coronary artery occlusion in human beings: echocardiographic observations during coronary angioplasty. *J Am Coll Cardiol*. 1985;5(2):193–7.
30. Wohlgeleit D, Cleman M, Highman HA, et al. Regional myocardial dysfunction during coronary angioplasty: evaluation by two-dimensional echocardiography and 12 lead electrocardiography. *J Am Coll Cardiol*. 1986;7(6):1245–54.
31. Seeberger MD, Skarvan K, Buser P, et al. Dobutamine stress echocardiography to detect inducible demand ischemia in anesthetized patients with coronary artery disease. *Anesthesiology*. 1998;88(5):1233–9.
32. Wang J, Filipovic M, Rudzitis A, et al. Transesophageal echocardiography for monitoring segmental wall motion during off-pump coronary artery bypass surgery. *Anesth Analg*. 2004;99(4):965–73.
33. Romero-Bermejo FJ, Ruiz-Bailen M, Gil-Cebrian J, Huertos-Ranchal MJ. Sepsis-induced Cardiomyopathy. *CCR*. 2011;7(3):163–83.
34. Chockalingam A. Acute left ventricular dysfunction in the critically ill. *Chest*. 2010;138(1):198.
35. Gudmundsson P, Rydberg E, Winter R, Willenheimer R. Visually estimated left ventricular ejection fraction by echocardiography is closely correlated with formal quantitative methods. *Int J Cardiol*. 2005;101(2):209–12.
36. Shahgaldi K, Gudmundsson P, Manouras A, Brodin L-Å, Winter R. Visually estimated ejection fraction by two dimensional and triplane echocardiography is closely correlated with quantitative ejection fraction by real-time three dimensional echocardiography. *Cardiovasc Ultrasound*. 2009;7(1):41.
37. Akinboboye O, Sumner J, Gopal A, et al. Visual estimation of ejection fraction by two-dimensional echocardiography: the learning curve. *Clin Cardiol*. 1995;18(12):726–9.
38. Skarvan K, Lambert A, Filipovic M, Seeberger M. Reference values for left ventricular function in subjects under general anaesthesia and controlled ventilation assessed by two-dimensional transesophageal echocardiography. *Eur J Anaesthesiol*. 2001;18(11):713–22.
39. Rouine-Rapp K, Ionescu P, Balea M, Foster E, Cahalan MK. Detection of intraoperative segmental wall-motion abnormalities by transesophageal echocardiography. *Anesth Analg*. 1996;83(6):1141–8.
40. Sherrid MV, Gunsburg DZ, Moldenhauer S, Pearle G. Systolic anterior motion begins at low left ventricular outflow tract velocity in obstructive hypertrophic cardiomyopathy. *J Am Coll Cardiol*. 2000;36(4):1344–54.
41. Wigle ED, Rakowski H, Kimball BP, Williams WG. Hypertrophic cardiomyopathy: clinical spectrum and treatment. *Circulation*. 1995;92(7):1680–92.
42. Clements FM, Harpole DH, Quill T, Jones RH, McCann RL. Estimation of left ventricular volume and ejection fraction by two-dimensional transoesophageal echocardiography: comparison of short axis imaging and simultaneous radionuclide angiography. *Br J Anaesth*. 1990;64(3):331–6.
43. Ryan T, Burwash I, Lu J, et al. The agreement between ventricular volumes and ejection fraction by transesophageal echocardiography or a combined radionuclear and thermodilution technique in patients after coronary artery surgery. *J Cardiothorac Vasc Anesth*. 1996;10(3):323–8.
44. Schmidlin D, Jenni R, Schmid ER. Transesophageal echocardiographic area and doppler flow velocity measurements: comparison with hemodynamic changes in coronary artery bypass surgery. *J Cardiothorac Vasc Anesth*. 1999;13(2):143–9.
45. Roysse CF. Ultrasound-guided haemodynamic state assessment. *Best Pract Res Clin Anaesthesiol*. 2009;23(3):273–83.

46. Cheung AT, Savino JS, Weiss SJ, Aukburg SJ, Berlin JA. Echocardiographic and hemodynamic indexes of left ventricular preload in patients with normal and abnormal ventricular function. *Anesthesiology*. 1994;81(2):376–87.
47. Greim CA, Roewer N, Apfel C, Laux G, am Esch JS. Relation of echocardiographic preload indices to stroke volume in critically ill patients with normal and low cardiac index. *Intensive Care Medicine*. 1997;23(4):411–6.
48. Swenson JD, Bull D, Stringham J. Subjective assessment of left ventricular preload using transesophageal echocardiography: corresponding pulmonary artery occlusion pressures. *J Cardiothorac Vasc Anesth*. 2001;15(5):580–3.
49. Tousignant CP, Walsh F, Mazer CD. The use of transesophageal echocardiography for preload assessment in critically ill patients. *Anesth Analg*. 2000;90(2):351.
50. Leung JM, Levine EH. Left ventricular end-systolic cavity obliteration as an estimate of intraoperative hypovolemia. *Anesthesiology*. 1994;81(5):1102–9.
51. Quiñones MA, Otto CM, Stoddard M, Waggoner A, Zoghbi WA. Recommendations for quantification of Doppler echocardiography: a report from the Doppler quantification task force of the nomenclature and standards committee of the American Society of Echocardiography. *J Am Soc Echocardiogr*. 2002;15(2):167–84.
52. Michard F, Teboul JL. Using heart-lung interactions to assess fluid responsiveness during mechanical ventilation. *Crit Care*. 2000;4(5):282–9.
53. Renner J, Broch O, Gruenewald M, et al. Non-invasive prediction of fluid responsiveness in infants using pleth variability index. *Anaesthesia*. 2011;66(7):582–9.
54. Feissel M. Respiratory changes in aortic blood velocity as an indicator of fluid responsiveness in ventilated patients with septic shock. *Chest*. 2001;119(3):867–73.
55. van Daele MERM, Trouwborst A, van Woerkens LCSM, Tenbrinck R, Fraser AG, Roelandt JRTC. Transesophageal echocardiographic monitoring of preoperative acute hypervolemic hemodilution. *Anesthesiology*. 1994;81(3):602–9.
56. Doi YL, Deanfield JE, McKenna WJ, Dargie HJ, Oakley CM, Goodwin JF. Echocardiographic differentiation of hypertensive heart disease and hypertrophic cardiomyopathy. *Heart*. 1980;44(4):395–400.
57. Maraud L, Gin H, Roudaut R, Aubertin J, Bricaud H. Echocardiographic study of left ventricular function in type 1 diabetes mellitus: hypersensitivity of β -adrenergic stimulation. *Diabetes Research and Clinical Practice*. 1991;11(3):161–8.
58. Hrovatin E, Piazza R, Pavan D, et al. Dynamic left ventricular outflow tract obstruction in the setting of acute anterior myocardial infarction: a serious and potentially fatal complication? *Echocardiography*. 2002;19(6):449–55.
59. Haley JH, Sinak LJ, Tajik AJ, Ommen SR, Oh JK. Dynamic left ventricular outflow tract obstruction in acute coronary syndromes: an important cause of new systolic murmur and cardiogenic shock. *Mayo Clinic Proceedings*. 1999;74(9):901–6.
60. GÖLbasi Z, Sakalli M, ÇİÇEK D, Aydogdu S. Dynamic left ventricular outflow tract obstruction in a patient with pheochromocytoma. *Jpn Heart J*. 1999;40(6):831–5.
61. Chandrasegaram MD, Celermajer DS, Wilson MK. Apical ballooning syndrome complicated by acute severe mitral regurgitation with left ventricular outflow obstruction—case report. *J Cardiothorac Surg*. 2007;2:14.
62. Brunetti ND, Ieva R, Rossi G, et al. Ventricular outflow tract obstruction, systolic anterior motion and acute mitral regurgitation in Tako-Tsubo syndrome. *Int J Cardiol*. 2008;127(3):e152–7.
63. Jebara VA, Mihaileanu S, Acar C, et al. Left ventricular outflow tract obstruction after mitral valve repair. Results of the sliding leaflet technique. *Circulation*. 1993;88(5 Pt 2):II30–34.
64. Aurigemma G, Battista S, Orsinelli D, Sweeney A, Pape L, Cuenoud H. Abnormal left ventricular intracavitary flow acceleration in patients undergoing aortic valve replacement for aortic stenosis. A marker for high postoperative morbidity and mortality. *Circulation*. 1992;86(3):926–36.

65. Auer J, Berent R, Weber T, Lamm G, Eber B. Catecholamine therapy inducing dynamic left ventricular outflow tract obstruction. *Int J Cardiol.* 2005;101(2):325–8.
66. Mingo S, Benedicto A, Jimenez MC, Pérez MA, Montero M. Dynamic left ventricular outflow tract obstruction secondary to catecholamine excess in a normal ventricle. *Int J Cardiol.* 2006;112(3):393–6.